Cluster expansion model for baryon number fluctuations in QCD

Volodymyr Vovchenko

ITP & FIAS, Goethe University Frankfurt, Germany

- Recent lattice QCD data at imaginary μ_B and role of baryonic interactions
- Radius of convergence of the Taylor expansion

V.V., A. Pásztor, S.D. Katz, Z. Fodor, H. Stoecker, Phys. Lett. B 775, 71 (2017)

V.V., J. Steinheimer, O. Philipsen, H. Stoecker, arXiv:1711.01261 [nucl-th]

Zimányi-COST Winter School on Heavy Ion Physics

Budapest, Hungary
December 8, 2017

Motivation: QCD equation of state at finite baryon density

Sketch of the QCD Phase Diagram

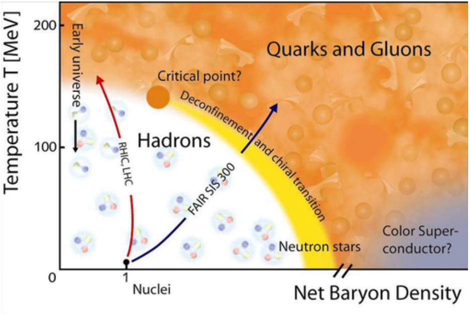

Lattice QCD EoS at $\mu_B = 0$

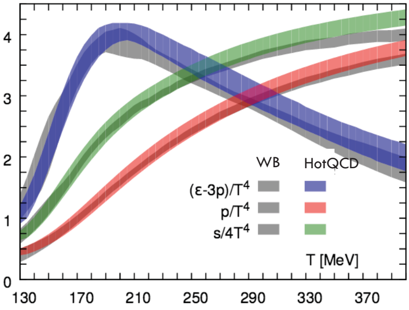

First-principle tool: Lattice QCD. Direct simulations restricted to $\mu_B = 0$.

What can we learn about EoS at finite μ_B from lattice and effective models?

Lattice-based methods for equation of state at finite μ_B

- Taylor expansion [Allton et al.; Gavai, Gupta; HotQCD Collaboration]

$$\frac{p(T,\mu_B)}{T^4} = \frac{p(T,0)}{T^4} + \frac{\chi_2^B(T,0)}{2!}(\mu_B/T)^2 + \frac{\chi_4^B(T,0)}{4!}(\mu_B/T)^4 + \dots$$

  χ_k^B – cumulants (susceptibilities) of net baryon distribution
  Can be computed in Lattice QCD at $\mu_B = 0$

- Analytic continuation from imaginary μ_B [de Forcrand, Philipsen; D'Elia, Lombardo]
  No sign problem at $\mu_B = i\tilde{\mu}_B$: Observables can be computed at $\mu_B^2 < 0$
  Then analytically continued to $\mu_B^2 > 0$
  Only few phenomenology studies: Quasiparticles [Bluhm, Kämpfer, PRD '08]; PQM [Morita et al., PRD '11]

- Other methods: Reweighting, complex Langevin, etc.

QCD observables at imaginary μ_B

QCD thermodynamics with relativistic fugacity/cluster expansion:

$$\frac{p(T,\mu_B)}{T^4} = \sum_{k=0}^{\infty} p_k(T) \cosh\left(\frac{k\,\mu_B}{T}\right)$$

Imaginary μ_B:

Lattice QCD is problematic at real μ but tractable at imaginary μ

$\mu_B \to \mathrm{i}\tilde{\mu}_B \quad \Rightarrow \quad$ QCD observables obtain trigonometric Fourier series form

Pressure: $$\frac{p(T,\mathrm{i}\tilde{\mu}_B)}{T^4} = \sum_{k=0}^{\infty} p_k(T) \cos\left(\frac{k\,\tilde{\mu}_B}{T}\right),$$

Net baryon density: $$\frac{\rho_B(T,\mathrm{i}\tilde{\mu}_B)}{T^3} = \mathrm{i}\sum_{k=1}^{\infty} b_k(T) \sin\left(\frac{k\,\tilde{\mu}_B}{T}\right), \quad b_k(T) \equiv k\,p_k(T)$$

$$b_k(T) = \frac{2}{\pi\,T^3}\int_0^{\pi} d\tilde{\mu}_B\,[\mathrm{Im}\,\rho_B(T,i\tilde{\mu}_B)]\,\sin(k\,\tilde{\mu}_B/T)$$

Coefficients $b_k(T)$ can and are now being calculated in LQCD

Expected asymptotics

- At low T/densities QCD thermodynamics $\simeq$ ideal hadron resonance gas

$$\frac{p^{\mathrm{hrg}}(T,\mu_B)}{T^4} = \frac{\phi_M(T)}{T^3} + 2\,\frac{\phi_B(T)}{T^3}\cosh\left(\frac{\mu_B}{T}\right),$$

$$\phi_B(T) = \sum_{i\in B}\int dm\,\rho_i(m)\,\frac{d_i\,m^2\,T}{2\pi^2}\,K_2\left(\frac{m}{T}\right),$$

$$p_0^{hrg}(T) = \frac{\phi_M(T)}{T^3},\quad p_1^{hrg}(T) = \frac{2\,\phi_B(T)}{T^3},\quad p_k^{\mathrm{hrg}}(T)\equiv 0,\ k=2,3,\ldots$$

- At high T QCD thermodynamics $\simeq$ ideal gas of massless quarks and gluons

$$\frac{p^{\mathrm{SB}}(T,\mu_B)}{T^4} = \frac{8\pi^2}{45} + \sum_{f=u,d,s}\left[\frac{7\pi^2}{60} + \frac{1}{2}\left(\frac{\mu_f}{T}\right)^2 + \frac{1}{4\pi^2}\left(\frac{\mu_f}{T}\right)^4\right],\quad \mu_f = \frac{\mu_B}{3}\,*,$$

$$p_0^{\mathrm{SB}} = \frac{64\pi^2}{135},\quad p_k^{\mathrm{SB}} = \frac{(-1)^{k+1}}{k^2}\,\frac{4\,[3+4\,(\pi k)^2]}{27\,(\pi k)^2},\quad b_k^{SB} = k\,p_k^{\mathrm{SB}}.$$

This work explores intermediate, transition region $130 < T < 230$ MeV

*In this study we assume that $\mu_S = \mu_Q = 0$

Lattice QCD results on imaginary μ_B observables

Coefficients $b_k(T)$ of net-baryon expansion are now calculated on the lattice

$$\frac{\rho_B(T, \mathrm{i}\tilde{\mu}_B)}{T^3} = \mathrm{i} \sum_{j=1}^{\infty} b_j(T) \sin\left(j\, \tilde{\mu}_B / T\right)$$

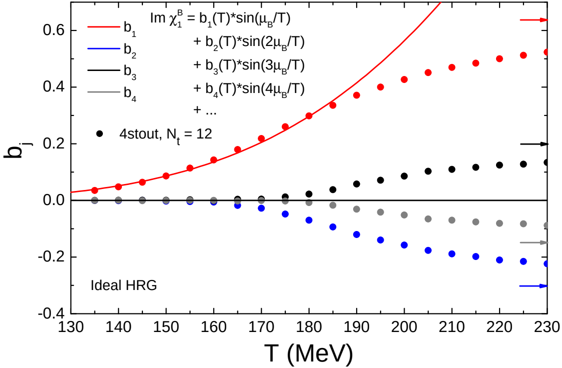

- Ideal HRG describes well $b_1(T)$ at small temperatures
- All four coefficients appear to converge slowly to Stefan-Boltzmann limit
- What is the mechanism of appearance of non-zero b_k for $k > 1$?

V.V., A. Pásztor, Z. Fodor, S.D. Katz, H. Stoecker, 1708.02852; S. Borsányi, QM2017

Reminder: Baryon susceptibilities and baryonic interactions

Onset of deviations of ideal HRG from LQCD captured by additions of attractive and repulsive van der Waals interactions between baryons

χ_{11}^{BQ}

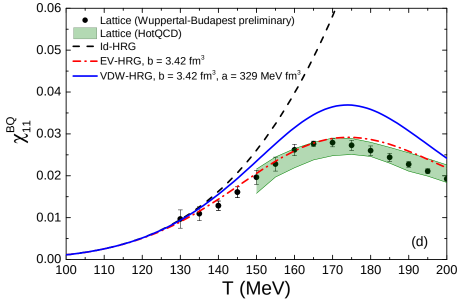

χ_4^B/χ_2^B

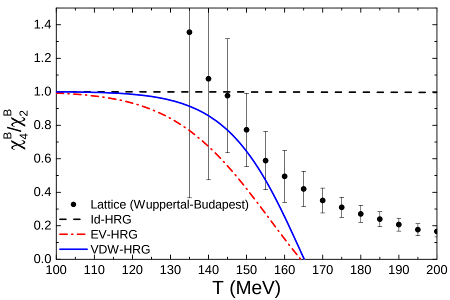

V.V., Gorenstein, Stoecker, Phys. Rev. Lett. 118, 182301 (2017) & Zimanyi School 2016
Some recent developments in the talk of P. Petreczky

Imaginary μ_B and repulsive baryonic interactions

Repulsive baryonic interactions with excluded-volume [Rischke et al., Z. Phys. C '91]

$$V \to V - bN \qquad \Rightarrow \qquad p_B(T,\mu_B) = p_B^{\rm id}(T, \mu_B - b p_B)$$

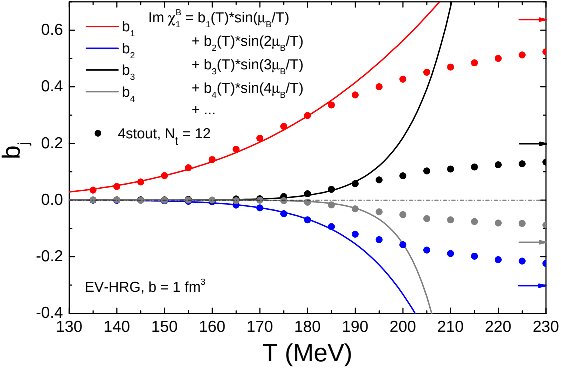

HRG with baryonic EV repulsion:

$$b_1^{\rm ev}(T) = 2\,\frac{\phi_B(T)}{T^3}$$

$$b_2^{\rm ev}(T) = -4\,[b\phi_B(T)]\,\frac{\phi_B(T)}{T^3}$$

$$b_3^{\rm ev}(T) = 9\,[b\,\phi_B(T)]^2\,\frac{\phi_B(T)}{T^3}$$

$$b_4^{\rm ev}(T) = -\frac{64}{3}\,[b\,\phi_B(T)]^3\,\frac{\phi_B(T)}{T^3}$$

- Ideal HRG describes well $b_1(T)$ at small temperatures
- Non-zero $b_j(T)$ for $j \geq 2$ signal deviations from ideal HRG
- EV interactions between baryons ($b \simeq 1$ fm^3) reproduces lattice trend

V.V., A. Pásztor, Z. Fodor, S. Katz, H. Stoecker, 1708.02852; S. Borsányi, QM2017

Relation between leading and higher order coefficients

EV-HRG describes similarly well leading four coefficients

A particular feature of the model: temperature-independent ratios

$$\alpha_3 = \frac{b_1(T)}{[b_2(T)]^2} b_3(T), \qquad \alpha_4 = \frac{[b_1(T)]^2}{[b_2(T)]^3} b_4(T), \qquad \ldots$$

Also hold true for many other models with short-range interaction

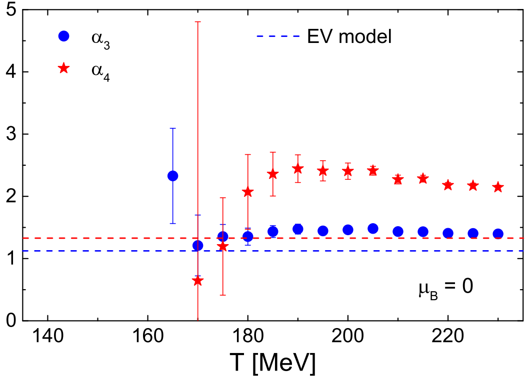

Excluded volume model:

$$\alpha_3^{EV} = 1.125, \quad \alpha_4^{EV} = 1.333$$

α_3 and α_4 are approximately T-independent on the lattice, EV somewhat off

Relation between leading and higher order coefficients

EV-HRG describes similarly well leading four coefficients

A particular feature of the model: temperature-independent ratios

$$\alpha_3 = \frac{b_1(T)}{[b_2(T)]^2} b_3(T), \qquad \alpha_4 = \frac{[b_1(T)]^2}{[b_2(T)]^3} b_4(T), \qquad \ldots$$

Also hold true for many other models with short-range interaction

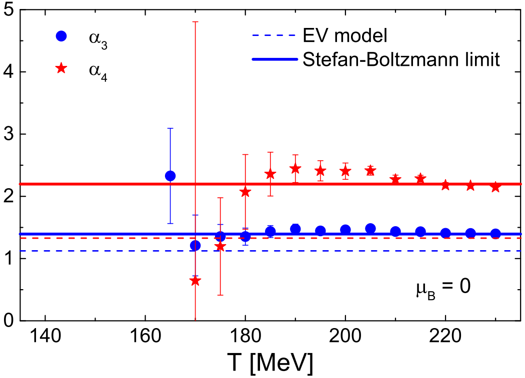

Excluded volume model:

$$\alpha_3^{EV} = 1.125, \quad \alpha_4^{EV} = 1.333$$

Stefan-Boltzmann limit:

$$\alpha_3^{SB} \simeq 1.394, \quad \alpha_4^{SB} \simeq 2.198$$

α_3 and α_4 are approximately T-independent on the lattice, EV somewhat off

Ratios are consistent with the Stefan-Boltzmann limit of massless quarks

Cluster Expansion Model (CEM)

α_3 and α_4 are consistent with SB limit. Now assume the same for all higher-order coefficients

CEM formulation:

- $b_1(T)$ and $b_2(T)$ are model input
- All higher order coefficients are then predicted

$$b_k(T) = \alpha_k^{SB} \frac{[b_2(T)]^{k-1}}{[b_1(T)]^{k-2}}$$

- All observables are calculated from fugacity expansion for baryon density

$$\frac{\rho_B(T)}{T^3} = \chi_1^B(T) = \sum_{k=1}^{\infty} b_k(T) \sinh(k\,\mu_B/T)$$

Fugacity expansion convergence criterion is given by the ratio test:

$$\lim_{k\to\infty} \left| \frac{b_{k+1}(T) \sinh\left[\frac{(k+1)\,\mu_B}{T}\right]}{b_k(T) \sinh\left[\frac{k\,\mu_B}{T}\right]} \right| = \left| \frac{b_2(T)\, b_1^{\mathrm{SB}}}{b_1(T)\, b_2^{\mathrm{SB}}} \right| e^{\frac{|\mu_B|}{T}} < 1.$$

V.V., J. Steinheimer, O. Philipsen, H. Stoecker, 1711.01261

CEM: Baryon number fluctuations

Baryon number susceptibilities at $\mu_B = 0$:

$$\chi_{2n}^B(T) \equiv \left.\frac{\partial^{2n}(p/T^4)}{\partial(\mu_B/T)^{2n}}\right|_{\mu_B=0} = \sum_{k=1}^{\infty} k^{2n-1}\, b_k(T) \simeq \sum_{k=1}^{k_{\max}} k^{2n-1}\, b_k(T).$$

CEM-LQCD: $b_1(T)$ and $b_2(T)$ taken from LQCD simulations at imaginary μ_B

V.V., J. Steinheimer, O. Philipsen, H. Stoecker, 1711.01261

CEM: Baryon number fluctuations

Baryon number susceptibilities at $\mu_B = 0$:

$$\chi_{2n}^B(T) \equiv \left. \frac{\partial^{2n}(p/T^4)}{\partial(\mu_B/T)^{2n}} \right|_{\mu_B=0} = \sum_{k=1}^{\infty} k^{2n-1}\, b_k(T) \simeq \sum_{k=1}^{k_{\max}} k^{2n-1}\, b_k(T).$$

CEM-LQCD: $b_1(T)$ and $b_2(T)$ taken from LQCD simulations at imaginary μ_B

χ_2^B

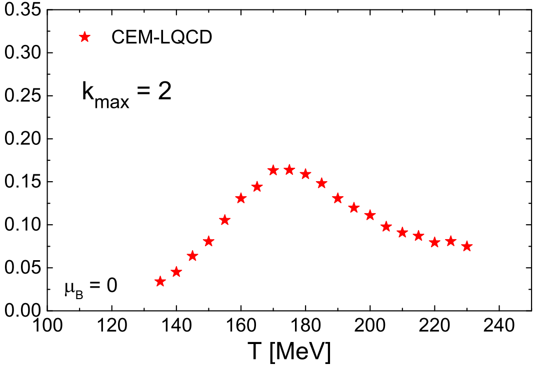

V.V., J. Steinheimer, O. Philipsen, H. Stoecker, 1711.01261

CEM: Baryon number fluctuations

Baryon number susceptibilities at $\mu_B = 0$:

$$\chi^B_{2n}(T) \equiv \left.\frac{\partial^{2n}(p/T^4)}{\partial(\mu_B/T)^{2n}}\right|_{\mu_B=0} = \sum_{k=1}^{\infty} k^{2n-1}\, b_k(T) \simeq \sum_{k=1}^{k_{\max}} k^{2n-1}\, b_k(T).$$

CEM-LQCD: $b_1(T)$ and $b_2(T)$ taken from LQCD simulations at imaginary μ_B

χ^B_2

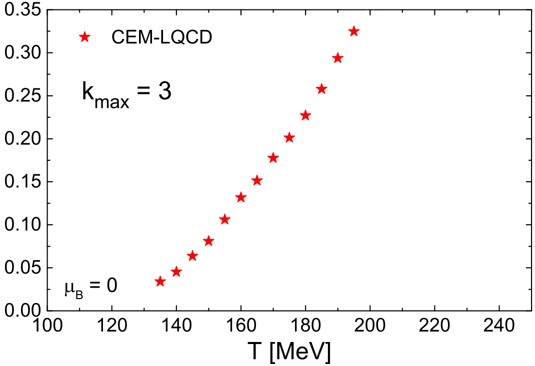

V.V., J. Steinheimer, O. Philipsen, H. Stoecker, 1711.01261

CEM: Baryon number fluctuations

Baryon number susceptibilities at $\mu_B = 0$:

$$\chi^B_{2n}(T) \equiv \left. \frac{\partial^{2n}(p/T^4)}{\partial(\mu_B/T)^{2n}} \right|_{\mu_B=0} = \sum_{k=1}^{\infty} k^{2n-1}\, b_k(T) \simeq \sum_{k=1}^{k_{\max}} k^{2n-1}\, b_k(T).$$

CEM-LQCD: $b_1(T)$ and $b_2(T)$ taken from LQCD simulations at imaginary μ_B

χ^B_2

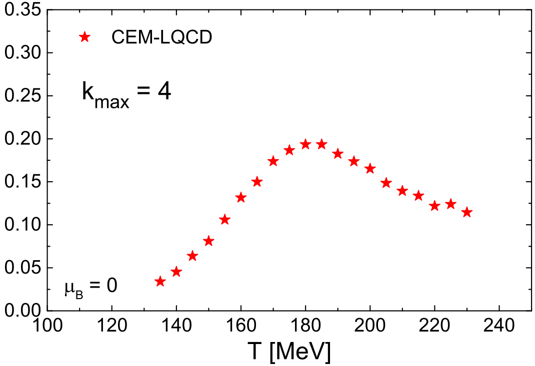

V.V., J. Steinheimer, O. Philipsen, H. Stoecker, 1711.01261

Baryon number susceptibilities at $\mu_B = 0$:

$$\chi_{2n}^{B}(T) \equiv \left.\frac{\partial^{2n}(p/T^4)}{\partial(\mu_B/T)^{2n}}\right|_{\mu_B=0} = \sum_{k=1}^{\infty} k^{2n-1}\, b_k(T) \simeq \sum_{k=1}^{k_{\rm max}} k^{2n-1}\, b_k(T).$$

CEM-LQCD: $b_1(T)$ and $b_2(T)$ taken from LQCD simulations at imaginary μ_B

χ_2^B

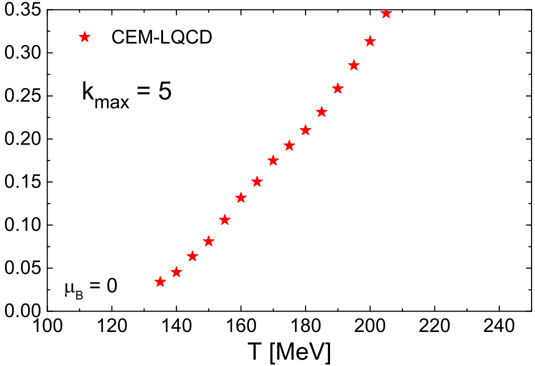

V.V., J. Steinheimer, O. Philipsen, H. Stoecker, 1711.01261

CEM: Baryon number fluctuations

Baryon number susceptibilities at $\mu_B = 0$:

$$\chi_{2n}^B(T) \equiv \left.\frac{\partial^{2n}(p/T^4)}{\partial(\mu_B/T)^{2n}}\right|_{\mu_B=0} = \sum_{k=1}^{\infty} k^{2n-1}\, b_k(T) \simeq \sum_{k=1}^{k_{\max}} k^{2n-1}\, b_k(T).$$

CEM-LQCD: $b_1(T)$ and $b_2(T)$ taken from LQCD simulations at imaginary μ_B

χ_2^B

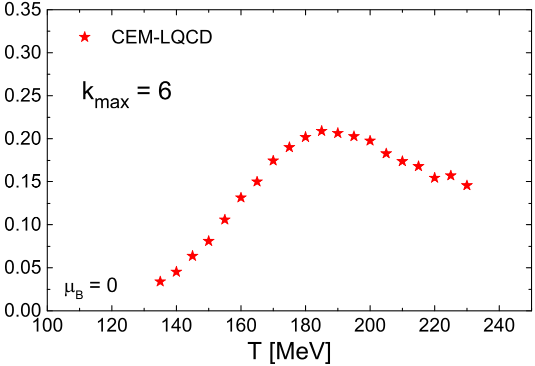

V.V., J. Steinheimer, O. Philipsen, H. Stoecker, 1711.01261

CEM: Baryon number fluctuations

Baryon number susceptibilities at $\mu_B = 0$:

$$\chi^B_{2n}(T) \equiv \left.\frac{\partial^{2n}(p/T^4)}{\partial(\mu_B/T)^{2n}}\right|_{\mu_B=0} = \sum_{k=1}^{\infty} k^{2n-1}\, b_k(T) \simeq \sum_{k=1}^{k_{\max}} k^{2n-1}\, b_k(T).$$

CEM-LQCD: $b_1(T)$ and $b_2(T)$ taken from LQCD simulations at imaginary μ_B

χ^B_2

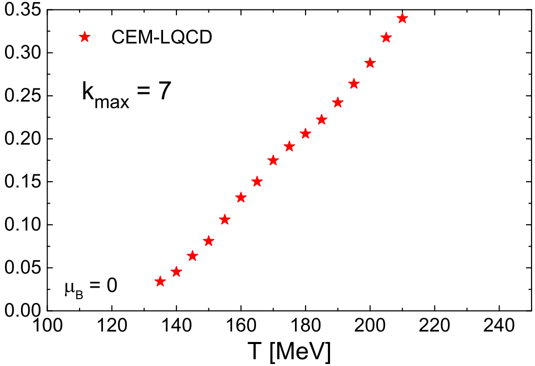

V.V., J. Steinheimer, O. Philipsen, H. Stoecker, 1711.01261

CEM: Baryon number fluctuations

Baryon number susceptibilities at $\mu_B = 0$:

$$\chi_{2n}^B(T) \equiv \left. \frac{\partial^{2n}(p/T^4)}{\partial(\mu_B/T)^{2n}} \right|_{\mu_B=0} = \sum_{k=1}^{\infty} k^{2n-1}\, b_k(T) \simeq \sum_{k=1}^{k_{\max}} k^{2n-1}\, b_k(T).$$

CEM-LQCD: $b_1(T)$ and $b_2(T)$ taken from LQCD simulations at imaginary μ_B

χ_2^B

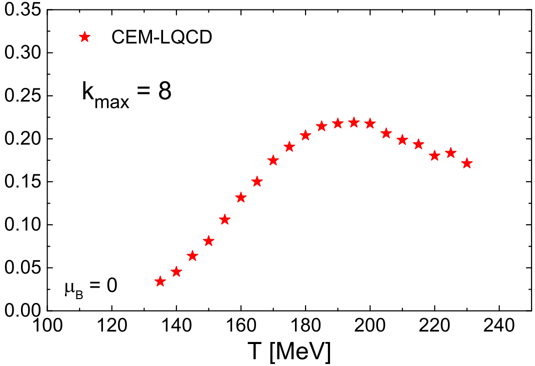

V.V., J. Steinheimer, O. Philipsen, H. Stoecker, 1711.01261

CEM: Baryon number fluctuations

Baryon number susceptibilities at $\mu_B = 0$:

$$\chi^B_{2n}(T) \equiv \left.\frac{\partial^{2n}(p/T^4)}{\partial(\mu_B/T)^{2n}}\right|_{\mu_B=0} = \sum_{k=1}^{\infty} k^{2n-1}\, b_k(T) \simeq \sum_{k=1}^{k_{\rm max}} k^{2n-1}\, b_k(T).$$

CEM-LQCD: $b_1(T)$ and $b_2(T)$ taken from LQCD simulations at imaginary μ_B

χ^B_2

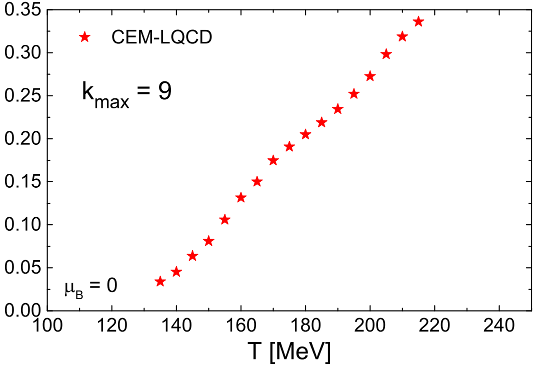

V.V., J. Steinheimer, O. Philipsen, H. Stoecker, 1711.01261

CEM: Baryon number fluctuations

Baryon number susceptibilities at $\mu_B = 0$:

$$\chi^B_{2n}(T) \equiv \left.\frac{\partial^{2n}(p/T^4)}{\partial(\mu_B/T)^{2n}}\right|_{\mu_B=0} = \sum_{k=1}^{\infty} k^{2n-1}\, b_k(T) \simeq \sum_{k=1}^{k_{\max}} k^{2n-1}\, b_k(T).$$

CEM-LQCD: $b_1(T)$ and $b_2(T)$ taken from LQCD simulations at imaginary μ_B

χ^B_2

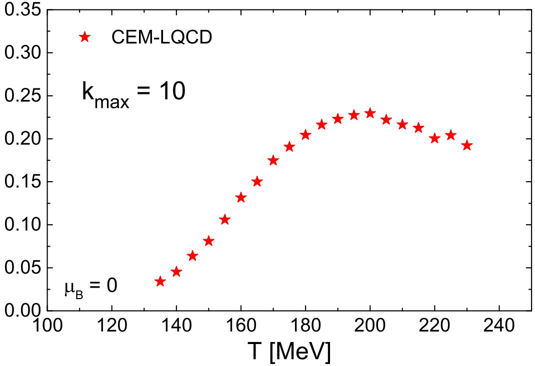

V.V., J. Steinheimer, O. Philipsen, H. Stoecker, 1711.01261

CEM: Baryon number fluctuations

Baryon number susceptibilities at $\mu_B = 0$:

$$\chi_{2n}^B(T) \equiv \left.\frac{\partial^{2n}(p/T^4)}{\partial(\mu_B/T)^{2n}}\right|_{\mu_B=0} = \sum_{k=1}^{\infty} k^{2n-1}\, b_k(T) \simeq \sum_{k=1}^{k_{\max}} k^{2n-1}\, b_k(T).$$

CEM-LQCD: $b_1(T)$ and $b_2(T)$ taken from LQCD simulations at imaginary μ_B

χ_2^B

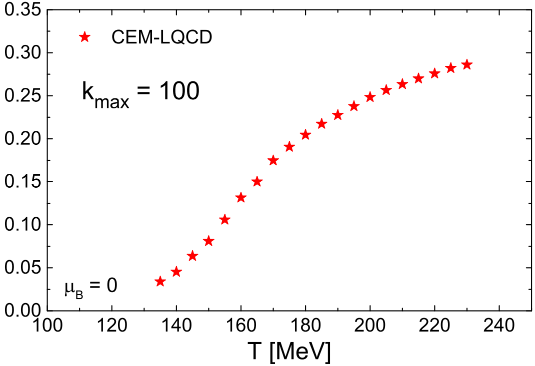

V.V., J. Steinheimer, O. Philipsen, H. Stoecker, 1711.01261

CEM: Baryon number fluctuations

Baryon number susceptibilities at $\mu_B = 0$:

$$\chi_{2n}^B(T) \equiv \left.\frac{\partial^{2n}(p/T^4)}{\partial(\mu_B/T)^{2n}}\right|_{\mu_B=0} = \sum_{k=1}^{\infty} k^{2n-1}\, b_k(T) \simeq \sum_{k=1}^{k_{\max}} k^{2n-1}\, b_k(T).$$

CEM-LQCD: $b_1(T)$ and $b_2(T)$ taken from LQCD simulations at imaginary μ_B

χ_2^B

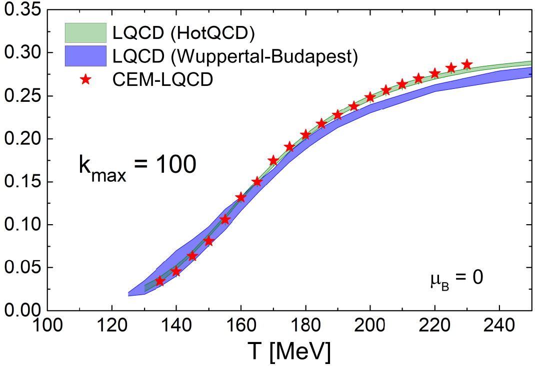

V.V., J. Steinheimer, O. Philipsen, H. Stoecker, 1711.01261

CEM: 4th and 6th order ratios

$$\chi_{2n}^B(T) \equiv \left.\frac{\partial^{2n}(p/T^4)}{\partial(\mu_B/T)^{2n}}\right|_{\mu_B=0} = \sum_{k=1}^{\infty} k^{2n-1}\, b_k(T).$$

χ_4^B/χ_2^B

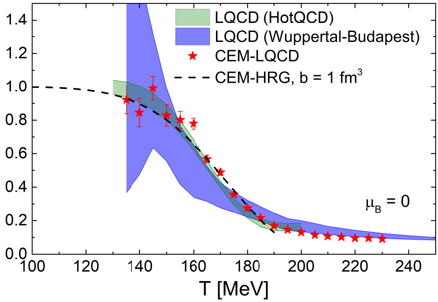

χ_6^B/χ_2^B

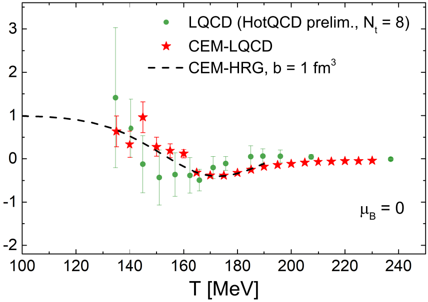

Consistency with available LQCD data

Hadronic description with interactions (CEM-HRG) works up to $T \simeq 185$ MeV

V.V., J. Steinheimer, O. Philipsen, H. Stoecker, 1711.01261
LQCD data from 1507.04627 (Wuppertal-Budapest), 1701.04325 & 1708.04897 (HotQCD)
CEM-HRG: $b_1(T)$ and $b_2(T)$ from EV-HRG model with $b = 1$ fm^3

CEM: predictions for high orders

$$\chi^B_{2n}(T) \equiv \frac{\partial^{2n}(p/T^4)}{\partial(\mu_B/T)^{2n}}\Big|_{\mu_B=0} = \sum_{k=1}^{\infty} k^{2n-1}\, b_k(T).$$

χ^B_8

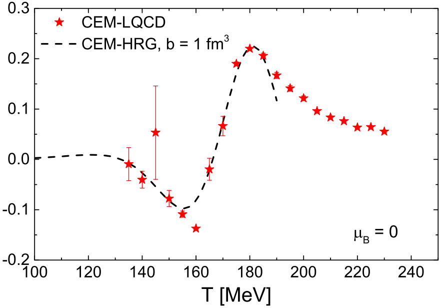

χ^B_{10}

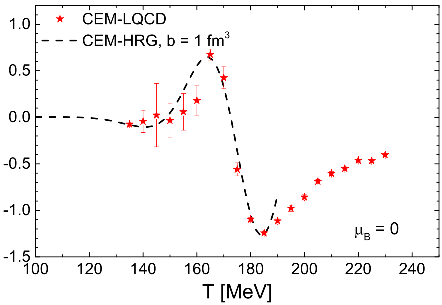

To be verified on the lattice

V.V., J. Steinheimer, O. Philipsen, H. Stoecker, 1711.01261

Radius of convergence

Taylor expansion of QCD pressure:

$$\frac{p(T,\mu_B)}{T^4} = \frac{p(T,0)}{T^4} + \frac{\chi_2^B(T)}{2!}(\mu_B/T)^2 + \frac{\chi_4^B(T)}{4!}(\mu_B/T)^4 + \dots$$

Radius of convergence $r_{\mu/T}$ of the expansion is the distance to the nearest singularity of p/T^4 in the *complex* μ_B/T plane at a given temperature T

If the nearest singularity is at a real μ_B/T value, this could point to the QCD critical point

Lattice QCD strategy: Estimate $r_{\mu/T}$ from few leading terms

M. D'Elia et al., 1611.08285; S. Datta et al., 1612.06673; A. Bazavov et al., 1701.04325

Ratio estimator: $r_n = \left| \frac{(2n+2)(2n+1)\chi_{2n}^B}{\chi_{2n+2}^B} \right|^{1/2}, \qquad r_{\mu/T} = \lim_{n\to\infty} r_n$

CEM allows to analyze r_n to very high order

Radius of convergence: Domb-Sykes plot

Domb-Sykes plot: $1/r_n^2$ vs $1/n$, linear extrapolation to $1/n = 0$ yields $r_{\mu/T}$

CEM-LQCD @ $T = 160$ MeV

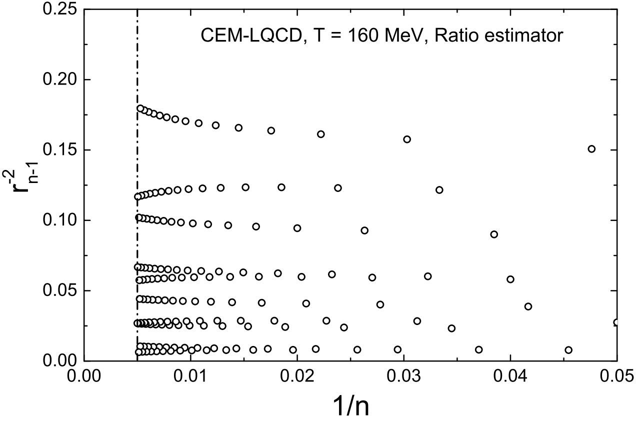

$$\lim_{n\to\infty} \left| \frac{(2n+2)(2n+1)\chi^B_{2n}}{\chi^B_{2n+2}} \right|^{1/2}$$ DOES NOT EXIST!

Radius of convergence: Structure of Taylor coefficients

Ratio estimator works only when coefficients have regular asymptotic structure: they either share the same sign or they alternate in sign

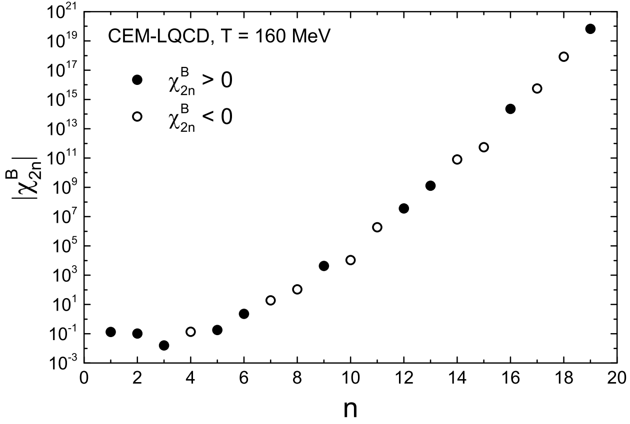

Negative coefficients appear from χ^B_8 on

Radius of convergence: Structure of Taylor coefficients

Ratio estimator works only when coefficients have regular asymptotic structure: they either share the same sign or they alternate in sign

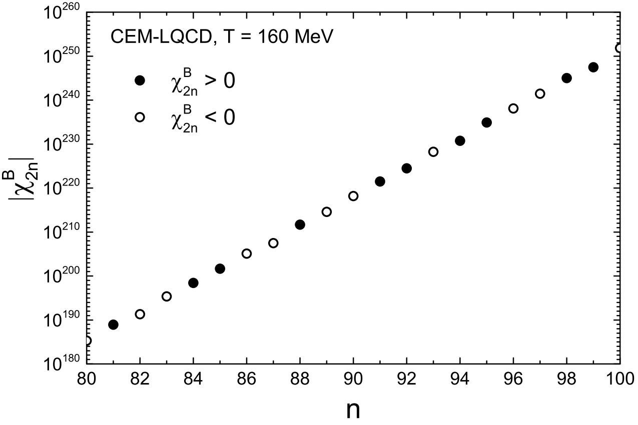

Negative coefficients appear from χ_8^B on

They never settle into a regular pattern

This means that limiting singularity lies in the *complex* μ_B/T plane

Radius of convergence: Mercer-Roberts estimator

A more involved Mercer-Roberts estimator:

$$r_n = \left| \frac{c_{n+1}\, c_{n-1} - c_n^2}{c_{n+2}\, c_n - c_{n+1}^2} \right|^{1/4}, \qquad c_n = \frac{\chi_{2n}^B}{(2n)!}.$$

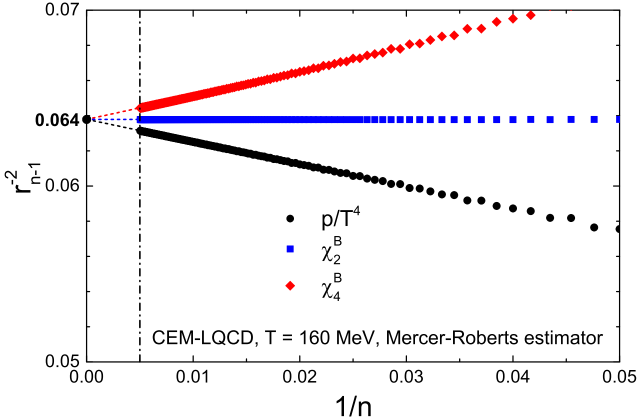

Taylor expansions for p/T^4, χ_2^B, and χ_4^B all point to the same

$$\lim_{n\to\infty} r_n^{-2} \simeq 0.064 \quad \Rightarrow \quad r_{\mu/T} \simeq 3.95 \text{ at } T = 160 \text{ MeV}$$

Radius of convergence: Temperature dependence

Applying the same procedure at other temperatures

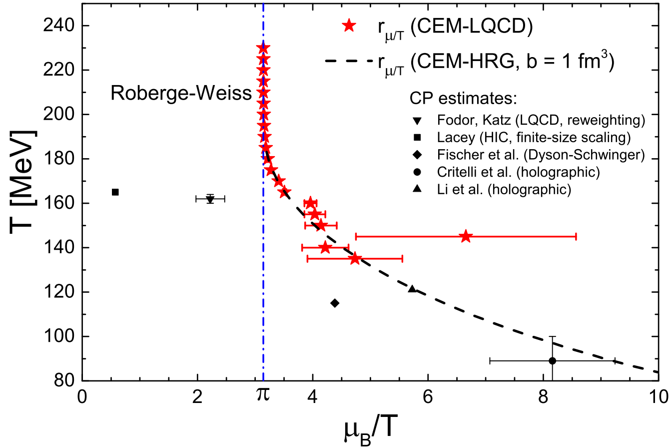

Radius of convergence of Taylor expansion sees Roberge-Weiss transition?

R-W transition expected at $T > T_{RW}$ and $\mathrm{Im}[\mu_B/T] = \pi$ [Roberge, Weiss, NPB '86]

Lattice estimate: $T_{RW} \sim 200$ MeV [C. Bonati et al., 1602.01426]

Radius of convergence: Cross-check with Padé approximants

Padé approximant for χ_2^B:

$$\chi_2^B(T, \mu_B/T) \approx \frac{\sum_{j=0}^{m} a_j \, (\mu_B/T)^j}{1 + \sum_{k=1}^{n} b_k \, (\mu_B/T)^k}$$

a_j and b_k constructed from χ_{2n}^B to match Taylor expansion

Poles of Padé approximants often point to true singularities of the function

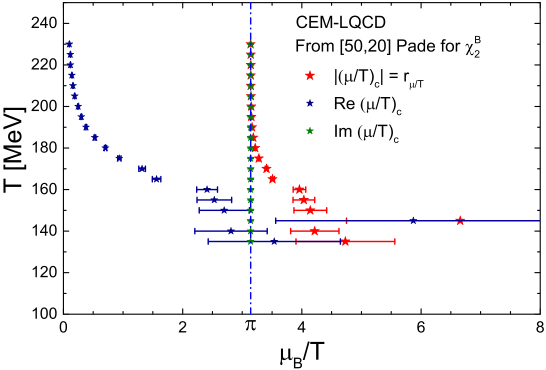

$\mathrm{Im}[\mu_B/T]_c = \pi$, while $\mathrm{Re}[\mu_B/T]_c$ decreases towards zero with temperature

Going beyond the radius of convergence

Padé approximants allow to go beyond the radius for convergence

Example: χ_4^B/χ_2^B at finite μ_B/T

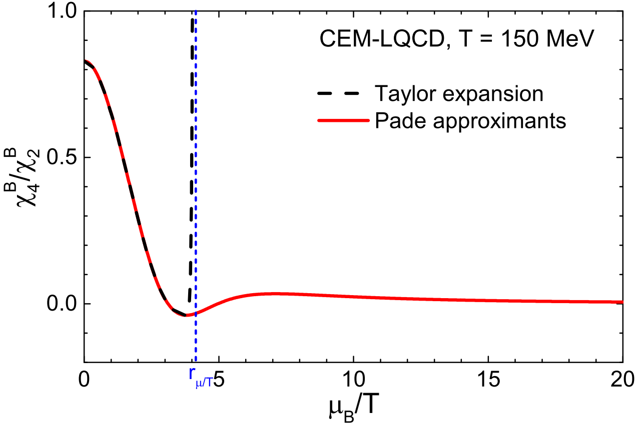

Summary

- LQCD data at imaginary μ_B suggests presence of repulsive baryonic interactions with 2nd virial coefficient $b \sim 1$ fm^3 in the crossover region
- It provides a first-principle evidence for the baryonic "excluded-volume"
- CEM describes all available lattice data on net baryon susceptibilities
- Radius of convergence of Taylor expansion sees a Roberge-Weiss like transition
- No evidence for QCD phase transition at $\mu_B/T < \pi$

Outlook

- QCD equation of state at finite μ_B/T within CEM
- Isospin and strangeness chemical potentials

Summary

- LQCD data at imaginary μ_B suggests presence of repulsive baryonic interactions with 2nd virial coefficient $b \sim 1$ fm^3 in the crossover region
- It provides a first-principle evidence for the baryonic "excluded-volume"
- CEM describes all available lattice data on net baryon susceptibilities
- Radius of convergence of Taylor expansion sees a Roberge-Weiss like transition
- No evidence for QCD phase transition at $\mu_B/T < \pi$

Outlook

- QCD equation of state at finite μ_B/T within CEM
- Isospin and strangeness chemical potentials

Thanks for your attention!

Backup slides

Baryonic excluded volume

Baryon-baryon interactions seem to exhibit a repulsive core – excluded volume

EV model: a simple approach for repulsive interactions [Rischke et al., Z. Phys. C '91]

$$V \to V - bN \qquad \Rightarrow \qquad p(T,\mu) = p^{\rm id}(T, \mu - bp)$$

EV-HRG model

- Identical EV interactions for all baryon-baryon and antibaryon-antibaryon pairs
- Baryon-antibaryon, meson-meson, meson-baryon EV terms neglected
- A single parameter b characterizing interactions

Three independent subsystems: mesons + baryons + antibaryons

$$p(T,\boldsymbol{\mu}) = p_M(T,\boldsymbol{\mu}) + p_B(T,\boldsymbol{\mu}) + p_{\bar{B}}(T,\boldsymbol{\mu}),$$

$$p_M(T,\boldsymbol{\mu}) = \sum_{j \in M} p_j^{\rm id}(T,\mu_j) \quad \text{and} \quad p_B(T,\boldsymbol{\mu}) = \sum_{j \in B} p_j^{\rm id}(T,\mu_j - b\, p_B)$$

Total density of baryons: $\quad n_B^{\rm ev} = (1 - b\, n_B^{\rm ev})\, e^{\mu_B/T}\, \phi_B(T) \exp\left(-\frac{b\, n_B^{\rm ev}}{1 - b\, n_B^{\rm ev}}\right).$

V.V., M. Gorenstein, H. Stoecker, Phys. Rev. Lett. 118, 182301 (2017)

L. Satarov, V.V., P. Alba, M. Gorenstein, H. Stoecker, Phys. Rev. C 95, 024902 (2017)

“Excluded volume” parameter from imaginary μ_B data

“Excluded volume” parameter of BB interactions can be estimated from lattice

$$b(T) = -\frac{b_2(T)}{[b_1(T)]^2\, T^3}$$

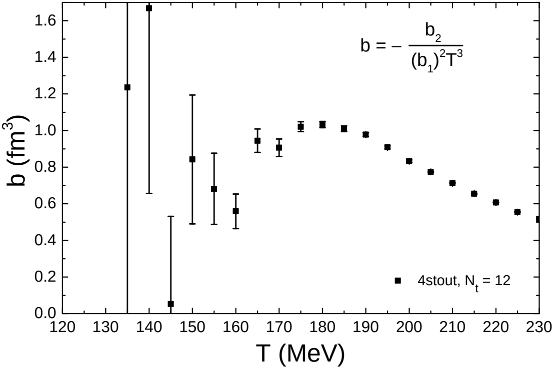

$b(T)$ mostly consistent with 1 fm^3 at $T < 190$ MeV

V.V., A. Pásztor, Z. Fodor, S.D. Katz, H. Stoecker, 1708.02852